Nano Energy 71 (2020) 104619

Contents lists available at ScienceDirect

Nano Energy

journal homepage: http://www.elsevier.com/locate/nanoen

Full paper

Genetic algorithm-driven discovery of unexpected thermal conductivity enhancement by disorder

Han Wei [a], Hua Bao [a,*], Xiulin Ruan [b,*]

[a] University of Michigan-Shanghai Jiao Tong University Joint Institute, Shanghai Jiao Tong University, Shanghai, 200240, China
[b] School of Mechanical Engineering and Birck Nanotechnology Center, Purdue University, West Lafayette, IN, 47907, USA

ARTICLE INFO

Keywords:
Porous graphene
Disorder
Thermal conductivity
Machine learning
Optimization

ABSTRACT

Discovering exceptions has been a major route for advancing sciences but a challenging and risky process. Machine learning has shown effectiveness in high throughput search of materials and nanostructures, but using it to discover exceptions has been out of the norm. Here we demonstrate the use of genetic algorithm to discover unexpected thermal conductivity enhancement in disordered nanoporous graphene as compared to periodic nanoporous graphene. Recent studies have concluded that random pores in nanoporous graphene lead to reduced thermal conductivity than periodic pores, due to phonon Anderson localization. This work, however, aims to challenge this accepted knowledge by searching for exceptions. A manual search was first shown to be expensive and unsuccessful. An efficient "two-step" search process coupled with genetic algorithm was then designed, and unexpected thermal conductivity enhancement was successfully discovered in certain structures with random pores, at a fraction of the computational cost of the manual search. Through structural analysis, we proposed that such unusual enhancement is due to the effect of shape factor and channel factor dominating over that of the phonon localization. Our work not only provides insights in thermal transport in disordered materials but also demonstrates the effectiveness of machine learning to discover small probability events and the intriguing physics behind.

1. Introduction

Discovering exceptions is a major route of advancing science. However, it is also a well-known highly risky process, since it usually involves a well-thought hypothesis, numerous trials and errors, but most often still ends with no success. Recently, on the other hand, the large amount of data generated by experiments and simulations have promoted the emergence of the "fourth paradigm"— (big) data science [1]. Studies have shown that the advanced data-driven paradigm can reproduce the existing physical laws based on data analysis only, for example, the heat diffusion equation and non-linear Navier-Stokes equations [2]. However, using machine learning to facilitate discoveries of exceptions beyond accepted knowledge is out of the norm. Here we consider thermal transport in disordered systems as a model problem.

Manipulating thermal transport in nanostructured materials [3–15] has attracted extensive research interest in thermal transport community for their promising applications in thermoelectric energy conversion [4,5,10,13], thermal insulation [3,14,15] and efficient heat dissipation [6,8,12]. Periodic nanostructures, including 1D superlattice [16–23] and 2D/3D phononic crystals [24–30], have been widely investigated, in which classical size effect [31,32] and wave interference [33,34] are two major mechanisms for modulating their thermal transport properties. Accordingly, disordered nanostructures also attracted significant research interest. It is found that, when there is no phonon coherence, the disorder has a negligible effect on the thermal conductivity. For example, experiments have shown that, at room temperature, the disordered and ordered nanoporous silicon membranes have the same value of thermal conductivity [35,36]. However, when phonon coherence occurs, a certain degree of disorder was found to effectively localize phonon propagation and thus reduce the thermal conductivity owing to the phonon localization [16,18,20–23,27,28,30,37–40]. For example, in 1D superlattice, aperiodic superlattice can achieve much lower thermal conductivity than the periodic superlattice [16,20,22,23] and even lower than the alloy limit [18,21]. Moreover, machine learning has recently been used to minimize the thermal conductivity of large scale 1D aperiodic superlattices and explain the physics behind [41]. In the 2D nanoporous graphene, the disorder of pore arrangement can reduce the thermal conductivity [27,28], and the

* Corresponding authors.
E-mail addresses: weihan2022@sjtu.edu.cn (H. Wei), hua.bao@sjtu.edu.cn (H. Bao), ruan@purdue.edu (X. Ruan).

https://doi.org/10.1016/j.nanoen.2020.104619
Received 5 January 2020; Received in revised form 7 February 2020; Accepted 12 February 2020
Available online 15 February 2020

amount of reduction can be up to 80% of the periodic counterpart [28]. In the 2D nanoporous C_3N, the reduction of thermal conductivity by the disordered pores was also observed [30].

It can be noted that all the results above were obtained by studying a limited number of disordered structures, despite the fact that there are infinite disordered structures for one system. Whether the limited sampled structures are representative enough has never been elucidated. Are there any exceptions to the conclusion? If so, is there a systematic and efficient way to identify them? In this work, we investigated the thermal transport in nanoporous graphene with disordered pore arrangements. In contrast to providing another evidence that disordered pores reduce thermal conductivity due to phonon localization, we attempted to challenge this well-accepted knowledge by looking for exceptions. Not to our surprise, a manual search was extremely expensive but unsuccessful. Therefore, we developed a genetic algorithm enabled two-step search process to efficiently handle the huge configuration space, and we were able to discover unexpected cases where thermal conductivity is enhanced by the disorder. Analyzing these unusual cases further allows us to identify two important descriptors for the pore arrangement, which are strongly correlated to the thermal conductivity.

2. Results and discussion

We consider a monolayer nanoporous graphene constructed by removing atoms from a rectangular pristine graphene sheet, as shown in Fig. 1a and b. The period L_0 and porosity are set as 4.6 nm and 25%, which makes phonon transport cover the coherent regime and thus facilitates wave interference. To eliminate the size effect of thermal conductivity for nanoporous graphene, 17 columns and 4 rows of periods (pores) are arranged in the x and y direction. Correspondingly, the simulation domain has width $W = 18.4$ nm, length $L = 88.2$ nm, and 68 pores in total. In order to obtain the thermal conductivity of the nanoporous graphene, the standard non-equilibrium molecular dynamics (NEMD) simulation (see Appendix) is employed.

2.1. Manual search

We first attempted a search for random structures with possibly higher thermal conductivities than the periodic structure by randomly shifting the pores, as shown in Fig. 1c. For each pore, the shift distance is D, which depends on the degree of disorder in the x and y directions. For each configuration, the degree of disorder can be quantified by the average shift distance D_{ave} over all 68 pores. We generated 21 disordered configurations by setting the maximum shift distance in the x and y direction. They are categorized into four groups: shift only in x, shift only in y, small shift in both x and y, and large shift in both x and y. More details can be found in the Supporting Information. For all 21 disordered configurations, the porosity, pore size, number, and shape are the same as the periodic configuration, while the only difference is the pore arrangement.

NEMD simulations are then performed to compute thermal conductivities at 300 K. We have tested the statistical uncertainty of NEMD simulation and found that it is smaller than 3% (see Supporting Information). Due to the small simulation uncertainty, we regarded the result of one simulation accurate enough and thus only performed one simulation for one configuration. The thermal conductivities of periodic and 21 disordered configurations are shown in Fig. 1d, where we can see that the thermal conductivity of the periodic configuration is 41.0 W/mK, which is close to the result of a similar simulation setup in Hu's study [28]. We note that for all 21 disordered configurations, the thermal conductivity values are considerably lower than that of the periodic structure. Therefore, through manual search, we did not find any disordered configuration with higher thermal conductivity than the periodic case. Such a result is consistent with the work by Hu et al., where they find disorder will reduce the thermal conductivity due to the phonon localization. The highest thermal conductivity of the 21 disordered configurations is 38.6 W/mK, which occurs when we only shift pores in x direction. This particular configuration is shown in Fig. 1e. One can see that such a configuration is only a small modification of the periodic configuration. Overall, we found that with shift only in the x direction, the thermal conductivities are about 5%–13% lower than that of periodic configuration. In comparison, for the other three groups, the thermal conductivities are both within the range of 24–30 W/mK, which are about 30%–40% lower than that of periodic configuration. From the results, it can be seen that introducing disorder in different directions can have different effects on the thermal conductivity.

The computational cost for our manual search is worth mentioning. It cost about 3200 core hours by NEMD simulation of each configuration (containing about 47000 atoms). Overall, 67200 core hours were spent in the manual search process for the 21 disordered configurations. This extremely time-consuming search method makes it difficult to further

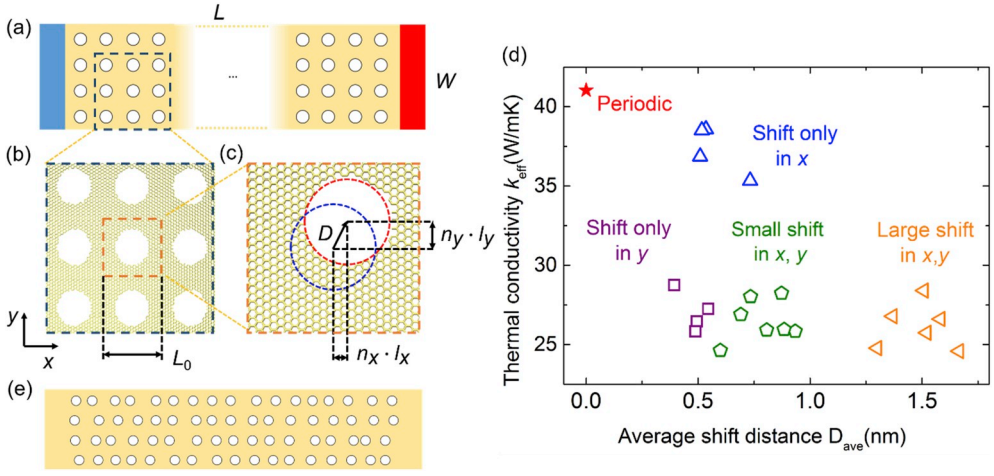

Fig. 1. The approach of generating disordered configurations and NEMD results in the manual search. (a) The schematic of NEMD simulation domain of nanoporous graphene with periodic pore arrangement. (b) The atomic configuration of nanoporous graphene with three periods in both x and y direction. The pores are situated at the center of periods with periodicity $L_0 = 4.6$ nm. (c) The enlarged figure of one period. The disordered porous structure is generated by shifting pores (denoted by the red circle) from the periodic positions (denoted by the blue circle) by a distance D. (d) Thermal conductivities of periodic and 21 disordered configurations. These configurations are categorized into four groups, which are distinguished using different colors. For example, "Shift in x" represents the configurations with pore shift only in x direction. "Large shift in x, y" represents the configurations with large pore shift in both x and y direction. (e) The schematic of disordered configuration with the highest thermal conductivity found in the manual search, which only has disorder in the x direction.

explore the sampling space.

2.2. Genetic algorithm enabled search

We realized that searching for the unlikely high-thermal-conductivity configuration by changing the shift of pores could be regarded as an optimization problem. The optimization variables are the degrees of disorder of pores and optimization target is the thermal conductivity. Inspired by the recent successful applications of machine learning algorithm [42–48], an efficient two-step search protocol is designed with an optimization algorithm. Among various optimization algorithms that have been developed, the genetic algorithm [49] (GA) has strong global optimization capabilities and convenient implementation, which have been successfully applied in material science and engineering [41,49–54]. Therefore, we chose to use GA for optimization in our search process.

From the perspective of optimization, our system has 136° of freedom. Considering the large computational cost of NEMD simulation, it is nearly impossible to conduct the optimization process even with the GA. To mitigate this problem, we need to further reduce the searching space and the computational cost for each sample. To reduce the searching space, the optimization is carried out with a reduced-size configuration with only 16 pores, as shown in Fig. 2a. Once an optimal configuration is found, the corresponding large-size configuration of 4 by 17 pore arrangement can be constructed by replicating the small-size configuration along the x direction. To reduce the computational cost for each configuration, we further choose to perform gray phonon BTE simulation to compute the thermal conductivities. Although phonon BTE can only consider particle transport characteristics of phonons (exclude wave effect) and the gray model neglect phonon modal details, it can still capture other effects of pore arrangement on the thermal conductivity[41, 42]. We identified a positive correlation between BTE and NEMD simulation results of the same configurations. More detailed can be found in Supporting Information. In comparison to NEMD, a single BTE simulation only cost 0.08 core hours on a reduced-size sample, which is basically negligible. Thus, BTE simulations can serve as a pre-screening tool. The details of gray BTE simulation can be found in Appendix. Of course, once a promising configuration is obtained with BTE, the case will be checked with NEMD, hence the accuracy is not sacrificed.

Fig. 2b presents the detailed workflow of the two-step search process. Starting from the periodic structure, 50 disordered reduced-size configurations are first generated, which are organized as the 1st generation. BTE simulations are then employed to compute the thermal conductivities. Through GA optimization, (i+1)-th generation are obtained by optimizing the i-th generation based on the computed thermal conductivities. After the optimization, the best individual that possesses the highest thermal conductivity in i-th generation is maintained in the (i+1)-th generation, which guarantees that the highest thermal conductivity for each generation could monotonically increase from the 1st generation. The convergence criterion is that the thermal conductivity of the best individual in each generation does not change over 8 generations [55,56]. If the GA optimization process is not converged, BTE simulation will be performed on the (i+1)-th generation and the same procedure will repeat. With converged results, NEMD simulations are finally applied to validate the thermal conductivities of corresponding large-size optimal configuration. If the NEMD result is not larger than the periodic configuration, then the entire search process will start over. Since our goal is to find one exception rather than all exceptions, we performed optimization on the configurations with disorder only in x or y direction rather than both directions.

Fig. 2c shows all the BTE computed normalized thermal conductivity k^* during the optimization process, in which the best individuals for each generation are shown as solid dots. We find that the best individuals for optimization in x and y direction increase from the 1st generation. Starting from a periodic configuration with normalized thermal conductivity of 3.97×10^{-3}, the evolutions converge at the 27-th and 24-th generation for optimization in x and y direction, respectively. The optimal normalized thermal conductivities are $4.27 \times 10^{-3}$and 4.35×10^{-3}, which are about 8% and 10% higher than that of

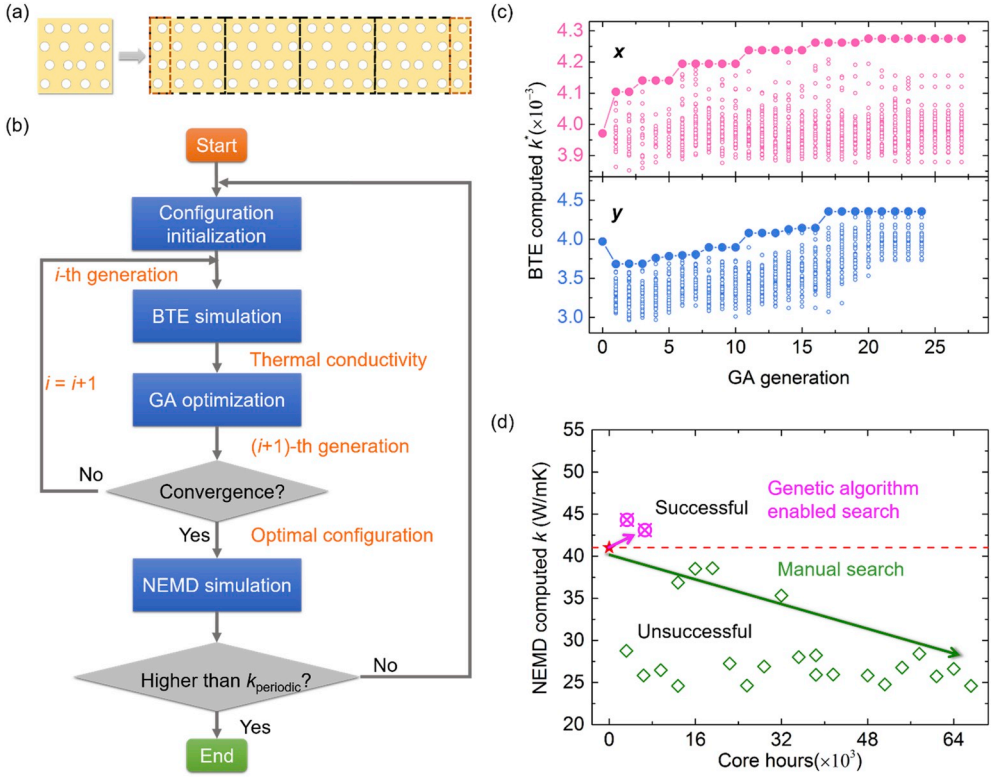

Fig. 2. The genetic algorithm enabled search process and optimization results. (a) The approach of constructing a large-size configuration of 4 by 17 pore arrangement from a reduced-size configuration with 4 by 4 pore arrangement. (b) The workflow of the two-step search process. BTE simulation is demonstrated for pre-screening and then NEMD simulation is performed to validate the optimal configuration found by GA. (c) The process of optimization for x and y direction, shown by the evolution of BTE computed normalized thermal conductivities with the GA generation. The small red (blue) circles denote the thermal conductivities of individuals in each generation, and the best individuals are denoted by the red (blue) solid dots. (d) The comparison of optimization output and the overall time cost between the genetic algorithm enabled search method and manual search method. 2 successful and 21 unsuccessful cases are distinguished using magenta and green colors.

the periodic configuration, respectively. For the two optimal configurations with disorder in x and y direction, the corresponding NEMD validated thermal conductivities are 44.3 W/mK and 43.1 W/mK, which are 8% and 5% higher than that of periodic configuration (41.0 W/mK). This enhancement is obviously larger than the statistical uncertainty of NEMD simulations and is accordingly a true enhancement. Therefore, this two-step search process successfully discovered an unexpected scenario, i.e., the thermal conductivity of disordered nanoporous graphene can be higher than the ordered counterpart. To our best knowledge, no such behavior has been reported in the literature yet.

The total computational cost needs to be highlighted. In this two-step search process, the computation cost for GA optimization is negligible, and thus the overall computational cost comes from BTE simulation and NEMD simulation. For BTE simulation, 1350 (=50 × 27) and 1200 (=50 × 24) configurations are computed for the optimization in x and y direction, which cost 204 (=2550 × 0.08) core hours in total. For NEMD simulation, two configurations are computed for validation, which cost 6400 (=3200 × 2) core hours. Therefore, about 6604 core hours were spent in this genetic algorithm enabled two-step search process. Compared to the manual search, our novel two-step search process proves to be very effective for our purpose of searching for exceptions. As summarized in Fig. 2d, in the unsuccessful manual search, about 67200 core hours were spent, while no disorder-enhanced case is found. For the successful genetic algorithm enabled search, with only 10% of the computation cost, two disorder-enhanced cases are found. Therefore, this genetic algorithm enabled two-step search strategy largely reduces the computational cost while increases the probability of success.

Similar to the optimization for high thermal conductivity, we can also perform optimization for low thermal conductivity. We note that thermal conductivities of randomly generated configurations with disorder in y direction are usually lower than that of with disorder in x direction. Therefore, the low thermal conductivity configuration is searched within the cases with disorder in y direction. The normalized thermal conductivity and NEMD computed thermal conductivity are 2.76×10^{-3} and 20.8 W/mK, respectively. The optimization results are included in the Supporting Information.

2.3. Structural analysis

Discovering the unexpected higher thermal conductivity in disordered porous graphene provides an exciting opportunity of understanding the intriguing physics behind it. It cannot be explained by the wave-like behaviors of phonons since the high thermal conductivity configuration is found in a disordered structure. We note that Maire et al. reported that at 4 K, the thermal conductivity of silicon nanoporous membranes can increase with some degree of disorder [36], and the authors attributed it to the randomness destroying the phonon bandgap in periodic structures hence allowing those phonons originally in the gap to contribute to heat transfer. Our system shows a different mechanism, otherwise, all our random configurations should have broken the phonon bandgap and easily shown enhanced thermal conductivity. We hypothesize that our enhancement of thermal conductivity of these two disordered configurations may be attributed to the particular pore arrangements that could enhance the particle-like transport of phonons. In order to understand how the pore arrangement can affect thermal conductivity, we inspect the four representative configurations: periodic configuration, two configurations with the highest thermal conductivity found in our genetic algorithm enabled two-step search, and also the configuration with lowest thermal conductivity. These configurations with BTE computed heat flux are shown in Fig. 3a, b, c, d. In the periodic configuration, the neck width [27] is small in the columns with pores and pretty large in the columns without pores. In comparison to the periodic configuration, we find that the highest thermal conductivity configuration with displacement only in x direction, shown in Fig. 3b, has a more uniform neck distribution in x direction, which originates from the more spread pore arrangement in the x direction. For the case with y direction displacements, the high thermal conductivity configuration, shown in Fig. 3c, has two wide channels between two different rows of pores. Whereas, in the low thermal conductivity configuration, shown in Fig. 3d, there is no clear channel and the pore arrangement in y direction is more spread compared to the configuration (c). Therefore, we expect the specific pore arrangement in x or y direction can have a significant influence on the thermal conductivity.

Inspired by such observation, we proposed two structural parameters—shape factor and channel factor, to describe the characteristics of pore arrangement in x and y direction. The concept of shape factor arises from the conduction shape factor used for determining the thermal resistance of 2D or 3D systems by the graphical method [57]. In the quasi-1D conduction scenario, as shown in Fig. 3e, the shape factor is defined as $S = 1/\int \frac{dx}{A(x)}$. For our nanoporous systems, $A(x)$ is related to the pore arrangement in x direction. Based on the definition, the configuration with more spread pore arrangement in x direction will have a larger shape factor. This means that pores belonging to different rows need to offset a certain amount. On the other hand, based on the observations, we proposed another parameter to describe the channels

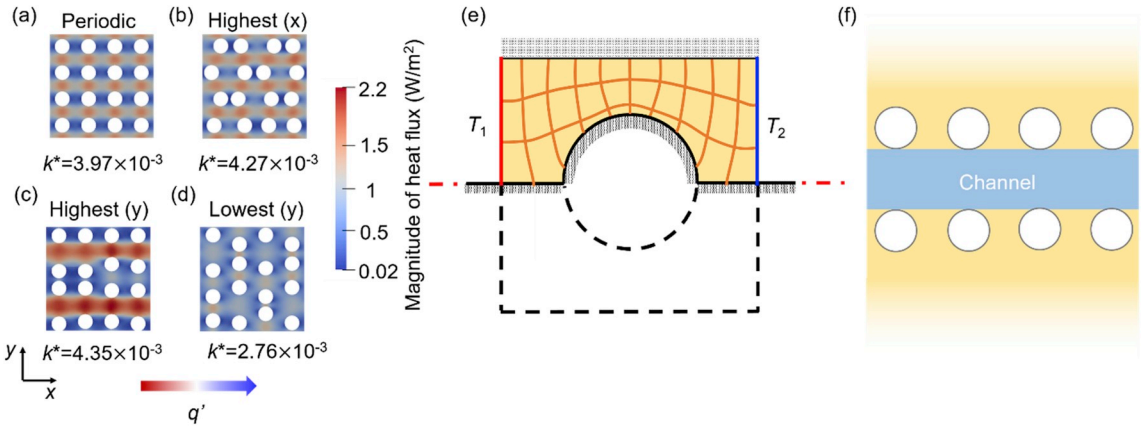

Fig. 3. The thermal transport in different nanoporous structures. The magnitude of BTE computed heat flux for (a) periodic configuration, (b), (c) the configuration with disorder in x and y direction identified by the GA optimization for high thermal conductivity, (d) the configuration with disorder in y direction identified by the GA optimization for low thermal conductivity. The corresponding thermal conductivity k^* are presented below the configurations and the color bar is shown beside. (e) The shape factor illustrated using a quasi-1D heat conduction scenario. The left red line and right blue line denote the isothermal boundary conditions with $T_1 > T_2$. The top, bottom, inner circle boundaries and symmetric lines are adiabatic. The orange lines represent isothermal and heat flow lines, delineated according to the boundary conditions. (f) The schematic of heat transfer channel, denoted by the blue region between two rows of pores.

existing between two rows of pores, as shown in Fig. 3f. We define the channel factor C as the standard deviation of $A(y)$, where $A(y)$ is related to the pore arrangement in y direction. Specifically, the configuration with a more spread pore arrangement in y direction will have a smaller channel factor.

By inspection of a few representative cases, we intuitively found that the thermal conductivity is closely related to pore arrangement, which can be quantified by shape factor and channel factor. However, it is still necessary to further examine whether these two structural parameters can be good descriptors for the thermal conductivities of disordered configurations. First, we verified the Pearson correlation coefficient [58] between the structural parameter and BTE computed thermal conductivities, which is usually used for the representing linear correlation between quantities. The corresponding values for shape factor and channel factor are 0.65 and 0.73, respectively. These results indicate good correlations between these two structural parameters and thermal conductivity. More details about the correlations between descriptors and thermal conductivities can be found in Supporting Information. Furthermore, we performed a regression analysis to find out the specific relationship between these two structural parameters and thermal conductivities. For this purpose, we choose the Least Square Regression (LSR) method [58–61], which has the special advantage of explicitly uncovering the relationship between the variables. The regression analysis strategy is shown in Fig. 4a. First, a dataset is generated including normalized thermal conductivities k^* of disordered configurations from BTE simulation and the corresponding shape factor S and channel factor C from structural analysis. To make the analysis more general, this dataset includes the configurations with disorder in either x or y direction and both two directions. Before regression, the dataset is randomly divided into a training set and test set, which is used for training the regression model and validating the prediction accuracy, respectively. We select 12 prototypical functions acting on the shape factor S and channel factor C to generate the basic components of the regression model, which are x,x^{-1}, $x^{1/2}$, $x^{-1/2}$, x^2, x^{-2}, x^3, x^{-3},ln(x), 1/ln(x), e^x, e^{-x}. With the training dataset, LSR is applied to establish the regression functions. Screening for the best ones is then demonstrated based on the coefficient of determination, which is commonly used for evaluating the prediction precision of regression function [1]. Two rounds of regression and screening are performed to formulate best the regression model $k^* = f(S, C)$. More details about regression analysis can be found in Supporting Information.

The final predictive model of normalized thermal conductivity as a function of the two structural parameters is given by:

$$k^* = 4.58 \times 10^{-3} - 5.30 \times 10^{-4} S^{-3} + 6.64 \times 10^{-2} C^3 \quad (1)$$

The predicted thermal conductivities of the training set and test set based on eq (1) are shown in Fig. 4b. The coefficient of determination of the prediction model for the training set and test set is 0.91 and 0.88, which shows that the prediction model can reasonably describe the relationship between the structural parameters and thermal conductivity. We finally compare the predicted normalized thermal conductivities and NEMD simulated thermal conductivities to evaluate the reliability of the prediction model. As shown in Fig. 4c, the predicted normalized thermal conductivities are still well correlated to the NEMD simulated thermal conductivity. The corresponding coefficient of determination is 0.78. Although small deviations appear, the overall consistency can still indicate that the structural parameters can effectively quantify the pore arrangement and be good descriptors for the thermal conductivity of nanoporous materials.

From eq (1), we can see that the normalized thermal conductivity increases with the increment of shape factor and channel factor. Combined these results with the definition of shape factor and channel factor, we found that a more spread pore arrangement in the x direction can enhance the thermal conductivity, while a more spread pore arrangement in the y direction can reduce the thermal conductivity. Therefore, the results of data analysis confirmed intuitive observations. This is a good example to show that with the help of machine-learning based method, new physical understanding of thermal transport can be discovered and validated.

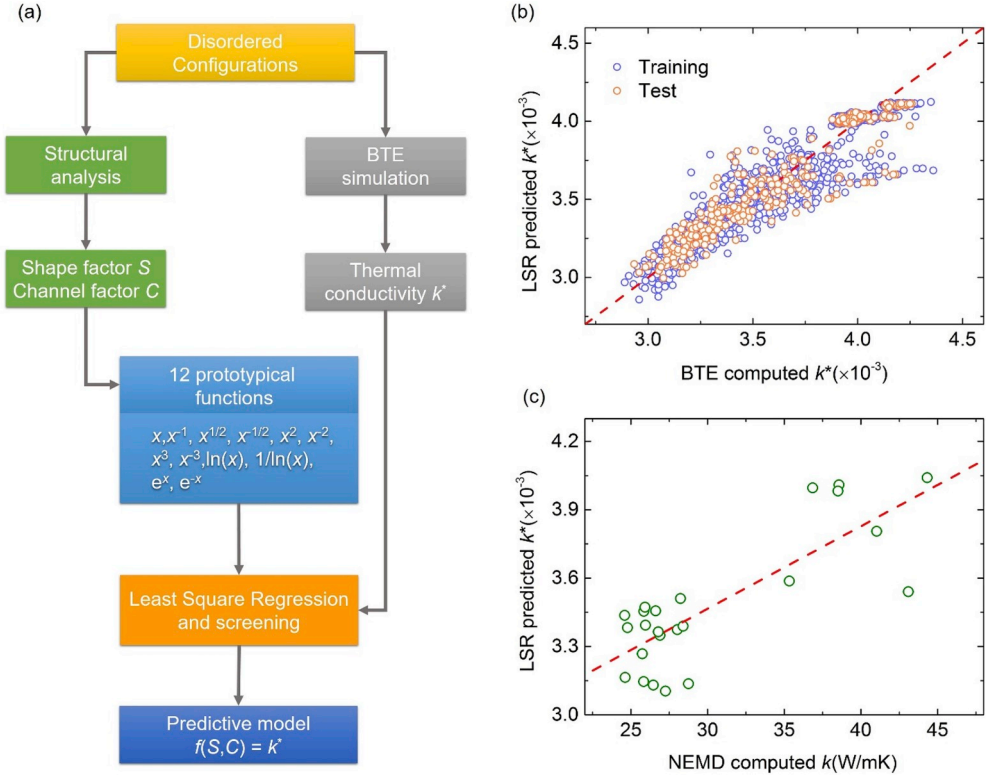

Fig. 4. Applying regression analysis for predicting the thermal conductivity of nanoporous graphene. (a) The schematic of the regression workflow for establishing the prediction model. The database is composed of thermal conductivities of disordered configurations and two structural parameters obtained from BTE simulation and structural analysis, respectively. The screening and regression processes are performed on the database and then a prediction model is obtained. (b) The comparison of thermal conductivity k^*calculated by BTE computation and the regression model. (c) The comparison of thermal conductivity k^*computed by MD computation and the machine-learning predicted thermal conductivity k.

3. Conclusion

In summary, we demonstrated an effective genetic algorithm-driven approach to discovering exceptions. Specifically, we investigated the thermal transport in disordered nanoporous graphene and attempted to find out disordered configuration with an unexpected higher thermal conductivity than the periodic counterpart. While the manual search was very expensive but unsuccessful, we proposed an efficient genetic algorithm enabled search method implemented with a "two-step optimization" strategy and discovered unexpected enhancement of thermal conductivity by disorder. Based on the structural analysis of the unusual cases, we proposed two parameters, shape factor and channel factor, to quantify the structural characteristics. The regression analysis further uncovered the relationship between the two structural parameters and thermal conductivities. We find that more spread pore arrangement in x direction can enhance the thermal conductivity, while more spread pore arrangement in y direction leads to lower thermal conductivity. Our findings not only provide new insight in thermal transport in 2D random nanoporous materials but also demonstrates the effectiveness of machine learning to assist the discovery of small probability events.

Declaration of competing interest

The authors declare that they have no known competing financial interests or personal relationships that could have appeared to influence the work reported in this paper.

Acknowledgement

This work is supported by Guangdong Province Key Area R&D Program (2019B010940001), the National Natural Science Foundation of China (No. 51676121), the Materials Genome Initiative Center of Shanghai Jiao Tong University and SJTU Zhiyuan Honor Ph.D. fellowship program. Simulations were performed with computing resources granted by HPC (π) from Shanghai Jiao Tong University. We thank Prabudhya Chowdhury for insightful discussions and Tianli Feng for his helpful guidance on the algorithms of generating structures.

Appendix

NEMD simulation. NEMD simulations involved in this paper are performed with the LAMMPS package [62]. Tersoff potential [63] is used to simulate the interatomic interactions among the carbon atoms. Fixed and periodic boundary conditions are applied along the length and width directions, respectively. Langevin thermostats with different temperatures are coupled with two ends of the simulation system to build up the temperature gradient along the thermal transport direction. The thermal conductivity is computed according to the Fourier's Law [64] based on the heat flux and temperature gradient in the steady state. More details about NEMD simulations are included in the Supporting Information.

BTE simulation. Boltzmann transport equation can describe phonon transport phenomenon and be used for solving ballistic heat conduction and obtain effective thermal conductivity of nanostructures [65–67]. Here we chose to solve the MFP-dependent BTE [68] numerically using the finite volume method and discrete ordinate method. All the simulations are performed with the OpenBTE package [68,69]. The only input of this computational framework is the bulk cumulative thermal conductivity [68]. More details about OpenBTE simulation details are included in the Supporting Information.

Genetic algorithm. Genetic algorithm is a global search algorithm based on the evolutionary principles of natural genetics and natural selection with the goal of optimizing a supplied fitness function [49]. In general, there are several processes involved in GA: population process, fitness calculation, selection and mutation [49]. More details about the GA optimization process are included in the Supporting Information.

Appendix A. Supplementary data

Supplementary data to this article can be found online at https://doi.org/10.1016/j.nanoen.2020.104619.

References

[1] A. Agrawal, A. Choudhary, Perspective: materials informatics and big data: realization of the "fourth paradigm" of science in materials science, Apl. Mater. 4 (5) (2016).
[2] A.B. Farimani, J. Gomes, V.S. Pande, Deep Learning the Physics of Transport Phenomena, 2017 [physics], 1709.02432.
[3] W.B. Gong, C.K. Sha, D.Q. Sun, W.Q. Wang, Microstructures and thermal insulation capability of plasma-sprayed nanostructured ceria stabilized zirconia coatings, Surf. Coating. Technol. 201 (6) (2006) 3109–3115.
[4] M.S. Dresselhaus, G. Chen, M.Y. Tang, R.G. Yang, H. Lee, D.Z. Wang, Z.F. Ren, J. P. Fleurial, P. Gogna, New directions for low-dimensional thermoelectric materials, Adv. Mater. 19 (8) (2007) 1043–1053.
[5] J.-H. Lee, G.A. Galli, J.C. Grossman, Nanoporous Si as an efficient thermoelectric material, Nano Lett. 8 (11) (2008) 3750–3754.
[6] P. Heino, Lattice-Boltzmann finite-difference model with optical phonons for nanoscale thermal conduction, Comput. Math. Appl. 59 (7) (2010) 2351–2359.
[7] A.A. Balandin, Thermal properties of graphene and nanostructured carbon materials, Nat. Mater. 10 (8) (2011) 569–581.
[8] D.L. Nika, A.A. Balandin, Two-dimensional phonon transport in graphene, J. Phys. Condens. Matter 24 (23) (2012) 233203.
[9] N. Yang, X. Xu, G. Zhang, B. Li, Thermal transport in nanostructures, AIP Adv. 2 (4) (2012), 041410.
[10] Y. Yan, Q.-F. Liang, H. Zhao, C.-Q. Wu, B. Li, Thermoelectric properties of one-dimensional graphene antidot arrays, Phys. Lett. 376 (35) (2012) 2425–2429.
[11] A.M. Marconnet, M.A. Panzer, K.E. Goodson, Thermal conduction phenomena in carbon nanotubes and related nanostructured materials, Rev. Mod. Phys. 85 (3) (2013) 1295–1326.
[12] Y. Xu, Z. Li, W. Duan, Thermal and thermoelectric properties of graphene, Small 10 (11) (2014) 2182–2199.
[13] J. Oh, H. Yoo, J. Choi, J.Y. Kim, D.S. Lee, M.J. Kim, J.-C. Lee, W.N. Kim, J. C. Grossman, J.H. Park, S.-S. Lee, H. Kim, J.G. Son, Significantly reduced thermal conductivity and enhanced thermoelectric properties of single- and bi-layer graphene nanomeshes with sub-10 nm neck-width, Nano Energy 35 (2017) 26–35.
[14] R. Ghasemi, H. Vakilifard, Plasma-sprayed nanostructured YSZ thermal barrier coatings: thermal insulation capability and adhesion strength, Ceram. Int. 43 (12) (2017) 8556–8563.
[15] S. Ju, T. Shiga, L. Feng, Z. Hou, K. Tsuda, J. Shiomi, Designing nanostructures for phonon transport via bayesian optimization, Phys. Rev. X 7 (2) (2017).
[16] F.X. Bronold, A. Alvermann, H. Fehske, Anderson localization in strongly coupled disordered electron–phonon systems, Phil. Mag. 84 (7) (2004) 673–704.
[17] J. Garg, N. Bonini, N. Marzari, High thermal conductivity in short-period superlattices, Nano Lett. 11 (12) (2011) 5135–5141.
[18] A. Frachioni, B.E.W. Jr, Simulated thermal conductivity of silicon-based random multilayer thin films, J. Appl. Phys. 112 (1) (2012), 014320.
[19] M.N. Luckyanova, J. Garg, K. Esfarjani, A. Jandl, M.T. Bulsara, A.J. Schmidt, A. J. Minnich, S. Chen, M.S. Dresselhaus, Z. Ren, E.A. Fitzgerald, G. Chen, Coherent phonon heat conduction in superlattices, Science 338 (6109) (2012) 936–939.
[20] Y. Wang, H. Huang, X. Ruan, Decomposition of coherent and incoherent phonon conduction in superlattices and random multilayers, Phys. Rev. B 90 (16) (2014) 165406.
[21] Y. Wang, C. Gu, X. Ruan, Optimization of the random multilayer structure to break the random-alloy limit of thermal conductivity, Appl. Phys. Lett. 106 (7) (2015), 073104.
[22] B. Qiu, G. Chen, Z. Tian, Effects of aperiodicity and roughness on coherent heat conduction in superlattices, Nanoscale Microscale Thermophys. Eng. 19 (4) (2015) 272–278.
[23] P. Chakraborty, L. Cao, Y. Wang, Ultralow lattice thermal conductivity of the random multilayer structure with lattice imperfections, Sci. Rep. 7 (1) (2017) 8134.
[24] P.E. Hopkins, C.M. Reinke, M.F. Su, R.H. Olsson, E.A. Shaner, Z.C. Leseman, J. R. Serrano, L.M. Phinney, I. El-Kady, Reduction in the thermal conductivity of single crystalline silicon by phononic crystal patterning, Nano Lett. 11 (1) (2011) 107–112.
[25] L. Yang, N. Yang, B. Li, Extreme low thermal conductivity in nanoscale 3D Si phononic crystal with spherical pores, Nano Lett. 14 (4) (2014) 1734–1738.
[26] S. Alaie, D.F. Goettler, M. Su, Z.C. Leseman, C.M. Reinke, I. El-Kady, Thermal transport in phononic crystals and the observation of coherent phonon scattering at room temperature, Nat. Commun. 6 (1) (2015) 7228.
[27] T. Feng, X. Ruan, Ultra-low thermal conductivity in graphene nanomesh, Carbon 101 (2016) 107–113.
[28] S. Hu, Z. Zhang, P. Jiang, J. Chen, S. Volz, M. Nomura, B. Li, Randomness-induced phonon localization in graphene heat conduction, J. Phys. Chem. Lett. 9 (14) (2018) 3959–3968.
[29] R. Anufriev, M. Nomura, Phonon and heat transport control using pillar-based phononic crystals, Sci. Technol. Adv. Mater. 19 (1) (2018) 863–870.
[30] S. Hu, Z. Zhang, P. Jiang, W. Ren, C. Yu, J. Shiomi, J. Chen, Disorder limits the coherent phonon transport in two-dimensional phononic crystal structures, Nanoscale 11 (24) (2019) 11839–11846.

[31] D. Song, G. Chen, Thermal conductivity of periodic microporous silicon films, Appl. Phys. Lett. 84 (5) (2004) 687–689.
[32] C. Huang, X. Zhao, K. Regner, R. Yang, Thermal conductivity model for nanoporous thin films, Phys. E Low-dimens. Syst. Nanostruct. 97 (2018) 277–281.
[33] M. Maldovan, Phonon wave interference and thermal bandgap materials, Nat. Mater. 14 (7) (2015) 667–674.
[34] G. Xie, D. Ding, G. Zhang, Phonon coherence and its effect on thermal conductivity of nanostructures, Adv. Phys. X 3 (1) (2018) 1480417.
[35] M.R. Wagner, B. Graczykowski, J.S. Reparaz, A. El Sachat, M. Sledzinska, F. Alzina, C.M. Sotomayor Torres, Two-Dimensional phononic crystals: disorder matters, Nano Lett. 16 (9) (2016) 5661–5668.
[36] J. Maire, R. Anufriev, R. Yanagisawa, A. Ramiere, S. Volz, M. Nomura, Heat conduction tuning by wave nature of phonons, Sci. Adv. 3 (8) (2017), e1700027.
[37] A. Kundu, A. Chaudhuri, D. Roy, A. Dhar, J.L. Lebowitz, H. Spohn, Heat conduction and phonon localization in disordered harmonic crystals, Europhys. Lett. 90 (4) (2010) 40001.
[38] I. Sarpkaya, E.D. Ahmadi, G.D. Shepard, K.S. Mistry, J.L. Blackburn, S. Strauf, Strong acoustic phonon localization in copolymer-wrapped carbon nanotubes, ACS Nano 9 (6) (2015) 6383–6393.
[39] M.N. Luckyanova, J. Mendoza, H. Lu, B. Song, S. Huang, J. Zhou, M. Li, Y. Dong, H. Zhou, J. Garlow, L. Wu, B.J. Kirby, A.J. Grutter, A.A. Puretzky, Y. Zhu, M. S. Dresselhaus, A. Gossard, G. Chen, Phonon localization in heat conduction, Sci. Adv. (2018) 11.
[40] T. Juntunen, O. Vänskä, I. Tittonen, Anderson localization quenches thermal transport in aperiodic superlattices, Phys. Rev. Lett. 122 (10) (2019).
[41] P. Roy Chowdhury, C. Reynolds, A. Garrett, T. Feng, S.P. Adiga, X. Ruan, Machine learning maximized Anderson localization of phonons in aperiodic superlattices, Nano Energy 69 (2020) 104428.
[42] Y. Liu, T. Zhao, W. Ju, S. Shi, Materials discovery and design using machine learning, J. Mater. 3 (3) (2017) 159–177.
[43] R. Ramprasad, R. Batra, G. Pilania, A. Mannodi-Kanakkithodi, C. Kim, Machine Learning and Materials Informatics: Recent Applications and Prospects, 2017 [cond-mat], 1707.07294.
[44] S. Ju, J. Shiomi, Materials informatics for heat transfer: recent progresses and perspectives, Nanoscale Microscale Thermophys. Eng. 23 (2) (2019) 157–172.
[45] Z. Pei, J. Yin, Machine learning as a contributor to physics: understanding Mg alloys, Mater. Des. 172 (2019) 107759.
[46] X. Wan, W. Feng, Y. Wang, H. Wang, X. Zhang, C. Deng, N. Yang, Materials discovery and properties prediction in thermal transport via materials informatics: a mini review, Nano Lett. (2019) acs.nanolett.8b05196.
[47] H. Wei, S. Zhao, Q. Rong, H. Bao, Predicting the effective thermal conductivities of composite materials and porous media by machine learning methods, Int. J. Heat Mass Tran. 127 (2018) 908–916.
[48] Q. Rong, H. Wei, X. Huang, H. Bao, Predicting the effective thermal conductivity of composites from cross sections images using deep learning methods, Compos. Sci. Technol. 184 (2019) 107861.
[49] D. Whitley, A genetic algorithm tutorial, Stat. Comput. 4 (2) (1994) 65–85.
[50] A. Konak, D.W. Coit, A.E. Smith, Multi-objective optimization using genetic algorithms: a tutorial, Reliab. Eng. Syst. Saf. 91 (9) (2006) 992–1007.
[51] R. Hu, T. Cheng, L. Li, J. Ma, X. Luo, Phosphor distribution optimization to decrease the junction temperature in white pc-LEDs by genetic algorithm, Int. J. Heat Mass Tran. 77 (2014) 891–896.
[52] M.-W. Li, D.-F. Han, W.-l. Wang, Vessel traffic flow forecasting by RSVR with chaotic cloud simulated annealing genetic algorithm and KPCA, Neurocomputing 157 (2015) 243–255.
[53] P.A. Avendaño, J.A. Souza, D.F. Adamatti, Construction of conductive pathways using genetic algorithms and constructal theory, Int. J. Therm. Sci. 134 (2018) 200–207.
[54] A. Kerr, K. Mullen, A comparison of genetic algorithms and simulated annealing in maximizing the thermal conductance of harmonic lattices, Comput. Mater. Sci. 157 (2019) 31–36.
[55] B. Lu, J. Wu, Z. Liang, C. Liu, Circuitry arrangement optimization for multi-tube phase change material heat exchanger using genetic algorithm coupled with numerical simulation, Energy Convers. Manag. 175 (2018) 213–226.
[56] R. Wu, X. Zhang, Y. Fan, R. Hu, X. Luo, A Bi-Layer compact thermal model for uniform chip temperature control with non-uniform heat sources by genetic-algorithm optimized microchannel cooling, Int. J. Therm. Sci. 136 (2019) 337–346.
[57] F.P. Incropera, Fundamentals of Heat and Mass Transfer, 1990.
[58] T. Zhan, L. Fang, Y. Xu, Prediction of thermal boundary resistance by the machine learning method, Sci. Rep. 7 (1) (2017) 7109.
[59] R. Liu, Y.C. Yabansu, A. Agrawal, S.R. Kalidindi, A.N. Choudhary, Machine learning approaches for elastic localization linkages in high-contrast composite materials, Integr. Mater. Manuf. Innov. 4 (1) (2015).
[60] A. Gupta, A. Cecen, S. Goyal, A.K. Singh, S.R. Kalidindi, Structure–property linkages using a data science approach: application to a non-metallic inclusion/steel composite system, Acta Mater. 91 (2015) 239–254.
[61] Z.-H. Shen, J.-J. Wang, J.-Y. Jiang, S.X. Huang, Y.-H. Lin, C.-W. Nan, L.-Q. Chen, Y. Shen, Phase-field modeling and machine learning of electric-thermal-mechanical breakdown of polymer-based dielectrics, Nat. Commun. 10 (1) (2019) 1843.
[62] S. Plimpton, Fast parallel algorithms for short-range molecular dynamics, J. Comput. Phys. 117 (1) (1995) 1–19.
[63] J. Tersoff, Modeling solid-state chemistry: interatomic potentials for multicomponent systems, Phys. Rev. B Condens. Matter 39 (8) (1989) 5566–5568.
[64] P.K. Schelling, S.R. Phillpot, P. Keblinski, Comparison of atomic-level simulation methods for computing thermal conductivity, Phys. Rev. B 65 (14) (2002) 144306.
[65] S. Zahiri, J. Zuo, Y. Shen, H. Bao, Numerical investigation of ballistic-diffusive heat transfer through a constriction with the Boltzmann transport equation, Appl. Therm. Eng. 141 (2018) 126–133.
[66] G. Romano, A.M. Kolpak, Diffusive Phonons in Nongray Nanostructures, 2017 [cond-mat], 1709.10199.
[67] G. Romano, A.M. Kolpak, J. Carrete, D. Broido, Parameter-free model to estimate thermal conductivity in nanostructured materials, Phys. Rev. B 100 (4) (2019), 045310.
[68] G. Romano, J.C. Grossman, Heat conduction in nanostructured materials predicted by phonon bulk mean free path distribution, J. Heat Tran. 137 (7) (2015), 071302.
[69] G. Romano, OpenBTE: a multiscale solver for the phonon Boltzmann transport equation, in: APS Meeting Abstracts, 2019. T70.321.

Han Wei is a Direct Ph. D student at University of Michigan-Shanghai Jiao Tong University Joint Institute. She received her B.S. in Energy and Power Engineering from Huazhong University of Science and Technology, China, in 2017. Her current research interests are in the machine learning and thermal transport in nanostructured materials.

Dr. Hua Bao is an associate professor at University of Michigan-Shanghai Jiao Tong University Joint Institute. He received his B.S. in Physics from Tsinghua University, China, in 2006, and his Ph.D. in Mechanical Engineering from Purdue University in 2012. His research interests are in micro/nano-scale thermal energy transport, thermophysical properties, and applications on thermal management and energy conversion.

Dr. Xiulin Ruan is a professor in the School of Mechanical Engineering and the Birck Nanotechnology Center at Purdue University. He received his B.S. and M.S. in Engineering Thermophysics from Tsinghua University in 2000 and 2002, respectively. He received an M.S. in Electrical Engineering and Ph.D. in Mechanical Engineering from the University of Michigan at Ann Arbor, in 2006 and 2007 respectively. His research interests are in multiscale multiphysics simulations and experiments of phonon, electron, and photon transport and interactions, for various emerging applications.